A self-consistent investigation of the semimetal–semiconductor transition in InAs/GaSb quantum wells under external electric fields

2004 J. Phys.: Condens. Matter 16 4677

(http://iopscience.iop.org/0953-8984/16/26/003)

INSTITUTE OF PHYSICS PUBLISHING JOURNAL OF PHYSICS: CONDENSED MATTER

J. Phys.: Condens. Matter **16** (2004) 4677–4684 PII: S0953-8984(04)76354-7

A self-consistent investigation of the semimetal–semiconductor transition in InAs/GaSb quantum wells under external electric fields

I Lapushkin[1], **A Zakharova**[1], **S T Yen**[2] **and K A Chao**[3]

[1] Institute of Physics and Technology of the Russian Academy of Sciences, Nakhimovskii Avenue 34, Moscow 117218, Russia
[2] Department of Electronics Engineering, National Chiao Tung University, Hsinchu, Taiwan, Republic of China
[3] Department of Physics, Lund University, Sölvegatan 14A, S 233 62 Lund, Sweden

Received 16 February 2004
Published 18 June 2004
Online at stacks.iop.org/JPhysCM/16/4677
doi:10.1088/0953-8984/16/26/003

Abstract

We investigate the phase transitions in InAs/GaSb quantum wells sandwiched between two wide-gap AlSb barrier layers under an external electric field perpendicular to interfaces. The Schrödinger and the Poisson equations are solved self-consistently to derive the subband dispersions, the potential profile, the electron charge distribution in the InAs layer, and the hole charge distribution in the GaSb layer. The Burt–Foreman envelope function theory and the scattering matrix method are used to solve the Schrödinger equation in the framework of the eight-band $\mathbf{k}\cdot\mathbf{p}$ model, including the spin-splitting of subbands in our calculation. We have found that in a thick InAs/GaSb quantum well, which has been investigated experimentally by Cooper *et al* (1998 *Phys. Rev.* B **57** 11915), under low external electric fields, two electron levels stay below the highest hole level at zero in-plane wavevector $\mathbf{k}_{\|} = 0$. Then, the anticrossings of electron and hole levels produce several minigaps in the in-plane dispersions, inside which the states of other subbands exist. As a result, the system is in a semimetal phase. With increasing external electric field, the semimetal phase changes to semiconductor phase with only one hybridization gap. When all electron levels become higher than the hole levels at higher electric fields, the system has a semiconducting gap.

1. Introduction

Whether the InAs/GaSb superlattices or quantum wells are in a semimetal phase or in a semiconducting phase has remained an interesting subject since the problem was first studied by Sai-Halasz *et al* [1]. In these structures, the electron affinity for InAs is larger than the sum of the electron affinity and energy gap for GaSb, so that the InAs conduction band overlaps

with the GaSb valence band. Because of this, the electrons can transfer through the InAs/GaSb interface from the GaSb valence band to the InAs conduction band, if the lowest electron level is below the highest hole level at zero in-plane wavevector $\mathbf{k}_\parallel = 0$. Such a system has been recognized to have semimetallic properties because of the existence of electron charge in InAs and hole charge in GaSb. Nevertheless, in 1983 Altarelli calculated the subband dispersions in the InAs/GaSb superlattices and found that the electron and hole levels anticross at some nonzero in-plane wavevector [2]. As a result of this anticrossing, a small hybridization gap opens, in the vicinity of which the conduction band-like subband and the valence band-like subband are formed with the positive and the negative effective masses, respectively. Recently, such a hybridization gap has been observed experimentally [3–8]. The electron–hole system with a positive direct gap [2, 8–15], inside which no state of other subbands exists, can exhibit semiconducting properties in spite of the possible coexistence of electron charge in InAs and hole charge in GaSb.

However, the spin-splitting phenomenon brings in an additional feature to the energy level structure. In structures with thick InAs and GaSb layers, the minigap between the lowest electron subband 1e and the highest heavy-hole subband 1hh with *up-spin* does not overlap with the minigap between the 1e subband and the 1hh subband with *down-spin* [14, 16]. Then the total gap is negative and indirect due to the large spin-splitting of levels, implying a semimetallic nature of the system. Further complication is caused by the geometric structure of the samples. In structures with a thick InAs layer in the absence of an external field, if the two lowest electron levels lie below the highest hole level at $\mathbf{k}_\parallel = 0$, different minigaps occur at different energies [8, 17]. Then, as demonstrated in [17], the states of one electron-like subband can exist inside the minigap between the other electron-like subband and the highest heavy-hole-like subband. Consequently, this system is in a semimetal phase. The quantum well of such type with a 30 nm InAs layer and a 15 nm GaSb layer was investigated experimentally [5], and the hybridization gap was probed by the resistance resonance in the four-terminal electrical transport measurements proposed in [10]. At low external bias across the InAs/GaSb quantum well, it was found that there is no resistance resonance due to the electron–hole hybridization. The authors explained this behaviour by the fact that the Fermi level is far from the hybridization gap. With increasing positive bias, the electron levels shift upwards and the hole levels shift downwards with respect to the conduction band edge at the centre of the quantum well structure, and so the Fermi level changes. At sufficiently high bias, the resistance resonance was found [5], resulting from the positive direct hybridization gap in the in-plane dispersion of the electron–hole system.

The rich physics connected with the electron–hole hybridization in InAs/GaSb quantum wells under an external electric field perpendicular to interfaces will be investigated in the present paper by solving self-consistently the Schrödinger and the Poisson equations using the realistic eight-band model [16]. In our calculations, we have used the scattering matrix method [18] and the Burt–Foreman envelope function theory [19, 20] (the details can be found in [16]). This approach allows us to treat subband dispersions in thick quantum wells which have been investigated experimentally [5]. We will obtain a new effect—a semimetal–semiconductor phase transition with the external electric field increasing. Previously the self-consistent calculation of the subband dispersions in the InAs/GaSb quantum wells, where the lowest electron level is below the highest hole level, were performed using only a simplified two-band model [10, 17] or the approach in which the electrons were treated in the one-band model while the holes were treated in the four-band model [11]. However, the semimetal–semiconductor phase transition under external electric fields was not considered in the previous calculations. The realistic eight-band model used in this work brings new features to subband dispersions caused by the spin-splitting of levels and electron–hole hybridization [14, 16].

The active region in our system is an InAs/GaSb quantum well sandwiched between two AlSb barriers. To simulate the potential profile, GaSb cap layers are added to each side of the active region. The purpose of our present theoretical investigation is to understand the experimental finding given in [5]. Hence, we specify our sample structure as the one used in the experiment with a 30 nm thick InAs layer and a 15 nm thick GaSb layer. Also, we take the thickness of each AlSb barrier equal to 10 nm and the acceptor concentration of 2×10^{17} cm^{-3} in the GaSb cap layers. To simplify our consideration we take the thicknesses of the AlSb barriers to be much smaller than those of experimental samples. The external electric field is created by applying a bias voltage between the two cap layers. An additional bias voltage applied to the InAs/GaSb channel controls the Fermi level position in the quantum well. Our calculation indicates that at a low electric field, the electron–hole system is in a semimetal phase with two minigaps in the in-plane dispersion. On increasing the field strength, the semimetal phase switches to a hybridized semiconducting phase with only one anticrossing gap. Further increase of the field results first in a zero-gap semiconductor phase, and then in the phase with a semiconducting gap when all electron levels are higher than the hole levels.

2. Self-consistent calculation scheme

To investigate the subband dispersions in the InAs/GaSb quantum well and the semimetal–semiconductor phase transition, we use the eight-band $\mathbf{k}\cdot\mathbf{p}$ model described in [16]. The [001] crystallographic direction is specified as the z-axis for quantization of spin and the angular momentum. The growth direction [010] is defined as the y-axis. To define the Hamiltonian matrix elements, we use the following set of basis functions: $u_1 = |s_{1/2,1/2}\rangle$, $u_2 = |p_{3/2,3/2}\rangle$, $u_3 = |p_{3/2,-1/2}\rangle$, $u_4 = |p_{1/2,-1/2}\rangle$, $u_5 = |s_{1/2,-1/2}\rangle$, $u_6 = |p_{3/2,-3/2}\rangle$, $u_7 = |p_{3/2,1/2}\rangle$, and $u_8 = |p_{1/2,1/2}\rangle$. Then, with the in-plane wavevector along the x-axis, the 8×8 $\mathbf{k}\cdot\mathbf{p}$ Hamiltonian $\hat{H}$ is block diagonalized as [16]

$$\hat{H} = \begin{pmatrix} \hat{H}_+ & 0 \\ 0 & \hat{H}_- \end{pmatrix}. \tag{1}$$

The two blocks $\hat{H}_\pm$ are given in [16]. They include as a parameter the potential profile in the quantum well.

Let ψ_i with $i = 1, 2, \ldots, 8$ be the envelope functions. If we define $\psi_+ = [\psi_1\psi_2\psi_3\psi_4]^{\mathrm{T}}$ and $\psi_- = [\psi_5\psi_6\psi_7\psi_8]^{\mathrm{T}}$, these envelope functions satisfy the equations

$$\hat{H}_\pm\psi_\pm = E\psi_\pm, \tag{2}$$

where E is an eigenvalue. Then the spin-polarized wavefunctions are $\Psi_+ = \sum_{i=1}^{4} u_i\psi_i$ for the *up-spin* states, and $\Psi_- = \sum_{i=5}^{8} u_i\psi_i$ for the *down-spin* states.

The energy level position depends on the potential distribution given by the Poisson equation

$$\frac{\mathrm{d}}{\mathrm{d}y}\varepsilon\frac{\mathrm{d}V(y)}{\mathrm{d}y} = 4\pi|e|\left[n(y) - p(y) - N_{\mathrm{D}}^{+} + N_{\mathrm{A}}^{-}\right], \tag{3}$$

where ε is the dielectric constant, e is the electronic charge, and N_{D}^{+}, N_{A}^{-}, n, and p are the concentrations of ionized donors, occupied acceptors, electrons, and holes, respectively. $V(y)$ is the potential distribution. The electron and hole concentrations in the quantum well are derived from the wavefunction distributions and the occupations of the states obtained in accordance with the Fermi–Dirac statistics.

The eigenvalue problem given by equation (2) is solved self-consistently with Poisson's equation by an iteration procedure. In each iteration, we solve first the Poisson equation taking

into account the charge accumulation in the quantum well. (The first iteration can be performed without charge in the well.) During this procedure, the potential shape is calculated using the Fermi energies E_{Fl} and E_{Fr} in the left and in the right GaSb contacts, which are controlled by the applied bias voltage between them and doping levels of contacts. The Fermi level in the quantum well E_{F} is taken as $E_{\mathrm{F}} = (E_{\mathrm{Fl}} + E_{\mathrm{Fr}})/2$. A Fermi level thus defined suggests that the applied bias between the left cap layer and the InAs/GaSb channel is equal to the applied bias between it and the right cap layer. The value of E_{F} can be changed by varying the voltages between the InAs/GaSb channel and the GaSb cap layers. Then equation (2) both for the *up-spin* and the *down-spin* states is solved as in [16] using the step-wise constant approximation for the obtained potential profile. The electron charge distribution and the hole charge distribution are derived using the calculated Fermi level position in the well with respect to the reference energy at the conduction band edge of its left boundary. When calculating the carrier charge distribution, we have neglected the very weak effect of the small subband anisotropy, as a commonly used approximation. When solving the Poisson equation, we have taken into account a donor defect concentration of 2×10^{11} cm^{-2} at the InAs/GaSb interface, according to the excess electron charges in the InAs/GaSb quantum wells observed experimentally [3, 5–7]. The donor defects are supposed to be totally ionized. The acceptor concentration is supposed to be zero. Using the obtained charge density distribution, the next iteration is performed. It gives us new solutions for carrier and potential distributions, subband dispersions, and wavefunctions. Self-consistent convergence is usually achieved after about fifteen iterations.

3. Results and discussion

The input parameters of materials, such as the energy band gaps, band offsets, and split-off energies, as well as the interband momentum matrix elements and the Luttinger parameters, are taken from [12]. While the effect of strain on subband dispersions has been investigated in our other works [14, 21], the influence of lattice-mismatched strain on the energy level structure is neglected here because of the strain relaxation on defects in the thick quantum well studied in this paper. All our numerical calculations are performed at the temperature 4.2 K.

We start with a low bias $V = 0.1$ V between the two cap layers. The self-consistent band edge profile is shown in panel (a) of figure 1. In panel (b) the electron density distribution in the InAs layer is plotted as a dashed curve, and the dotted curve is for the hole density distribution in the GaSb layer. The calculated total electron density in the InAs region is about 10^{12} cm^{-2}, but the calculated total hole density in the GaSb region is only about 1.5×10^{11} cm^{-2}. The excess of electrons in the well is due to the ionization of donor defects in the well and the injection of electrons from the contacts into the well. Because of this large net electron concentration in the InAs layer, the local electric field is considerably screened, indicating a weak band bending in the InAs layer except for the region adjacent to the InAs/GaSb boundary as shown in figure 1(a).

The subband dispersions at $V = 0.1$ V are shown in figure 2 with solid curves for the *up-spin* states and dashed curves for the *down-spin* states. The Fermi level is marked with a dotted line. At the zone centre ($\mathbf{k}_{\parallel} = 0$), the two energy levels corresponding to the *up-spin* and *down-spin* states coincide due to the time reversal symmetry. In this situation, the seven subbands can be unambiguously labelled as 1e, 2e, and 3e for the electron states, 1hh, 2hh, and 3hh for the heavy-hole states, and 1lh for the light-hole states. Since at $\mathbf{k}_{\parallel} = 0$ the lowest electron level 1e lies below the heavy-hole levels 1hh and 2hh, as well as below the light-hole level 1lh, at finite values of $\mathbf{k}_{\parallel}$, multiple anticrossings occur between the electron-like states and the hole-like states, producing multiple minigaps. We can see clearly that because of the

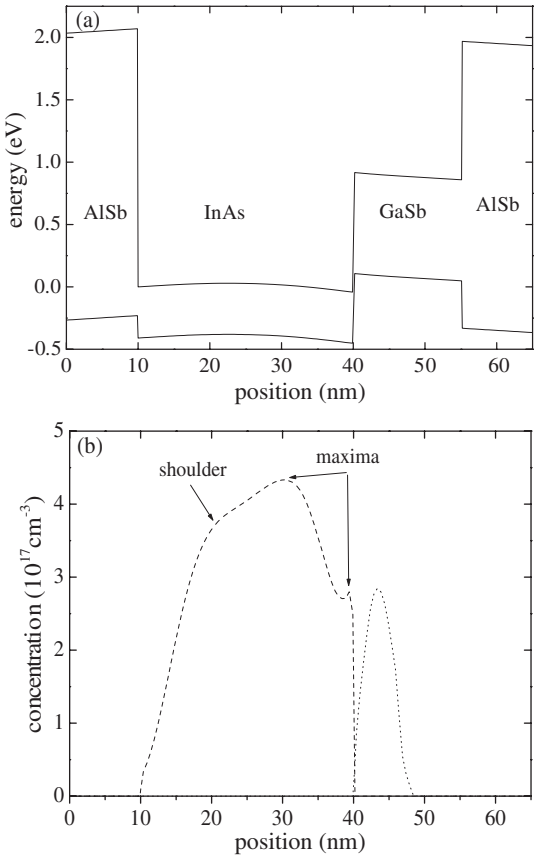

Figure 1. (a) Conduction and valence band profile of the AlSb/InAs/GaSb/AlSb quantum well structure with a 30 nm InAs layer and a 15 nm GaSb layer under a bias of 0.1 V, and (b) electron and hole distributions shown by dashed and dotted curves, respectively.

spin-splitting of subbands, the minigap between the 1e-like and 1hh-like subbands is negative and indirect. On the other hand, at $\mathbf{k}_\parallel = 0$, the 2e level lies below only the 1hh hole level. Hence, at $k_\parallel = 0.05$ nm^{-1} the anticrossing generates a positive and direct hybridization gap of about 1 meV. Since this minigap overlaps with the states in the 1e-like subband, no true energy gap exists at the bias $V = 0.1$ V, and the electron–hole system is in a semimetal phase.

The spatial distribution of the carrier density shown in figure 1(b) is calculated from the occupied states in figure 2. The electron density in figure 1(b) has two maxima and a shoulder. The left maximum comes from the electrons in the 1e subband while the electrons in the 2e subband contribute to the other maximum and the shoulder. The hole concentration has only one maximum since only the 1hh level is occupied by holes.

To illustrate the importance of the electron screening, we repeat our calculation based on the independent-electron picture by removing the Coulomb interaction between all charge carriers. The subband dispersions thus obtained are plotted in figure 3. Contrary to figure 2, the lowest electron level 1e in figure 3 is strongly mixed with the second light-hole level 2lh at zero in-plane wavevector, giving rise to two mixed 1e–2lh levels. In figure 3, only the higher mixed 1e–2lh level is shown. The lower one, slightly below the conduction band edge of the left InAs layer boundary, is beyond the scale of the figure and is not shown here. The Fermi

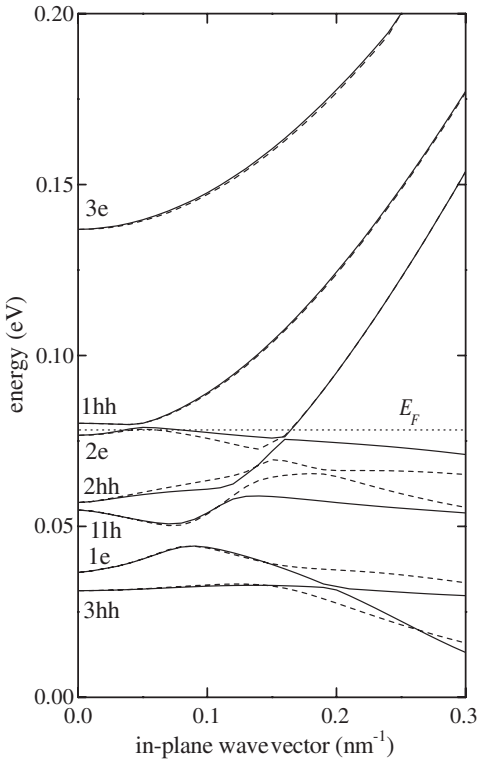

Figure 2. Subband dispersions and the Fermi level for the AlSb/InAs/GaSb/AlSb quantum well structure with a 30 nm InAs layer and a 15 nm GaSb layer at a bias of 0.1 V. Solid and dashed curves correspond to the *up-spin* and *down-spin* states, respectively. The dotted line is shown as the Fermi level.

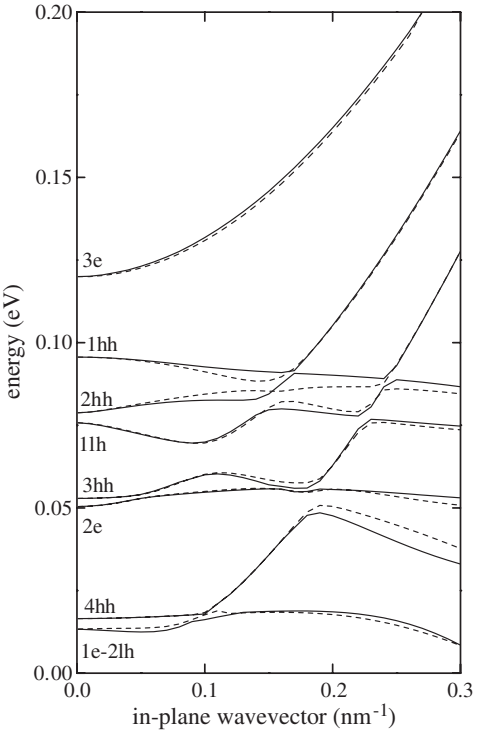

Figure 3. Subband dispersions as in figure 2 but without the Coulomb interaction among charge carriers.

level position in the well with respect to the reference energy has not been calculated in the non-self-consistent scheme, and hence has not been shown in figure 3. By comparing figures 2 and 3, we see that the neglect of the interaction between charge carriers can cause an error as large as 25 meV in the energy level structure.

Electrons and holes respond differently to the external electric field, and their subband dispersions are sensitive to the applied bias. When the bias is increased to $V = 0.25$ V, the dispersions change from those in figure 2 to those in figure 4. We see that at $\mathbf{k}_\parallel = 0$, the general feature is the down shift of the hole levels with respective to the electron levels. For the present case, the 1e-like subband lies just below the 1hh-like subband at small values of $k_\parallel$. The hybridization gap between the 1e subband and the 1hh subband, derived from our calculation, is about 1 meV for the *up-spin* states and about 2.5 meV for the *down-spin* states. The calculated average gap of about 1.75 meV is in a good agreement with the anticrossing gap of 2 meV detected in experiment [5]. The electron–hole system with a positive hybridization gap is in a semiconducting phase. Hence, the semimetal–semiconductor phase transition has taken place as the bias changes from $V = 0.1$ to 0.25 V. Such a phase transition has been observed experimentally [5].

With further increase of bias, the energy levels 1e and 1hh at $\mathbf{k}_\parallel = 0$ will merge, and the zero-gap semiconducting phase is reached. We found this phase at $V \simeq 0.3$ V. When the bias

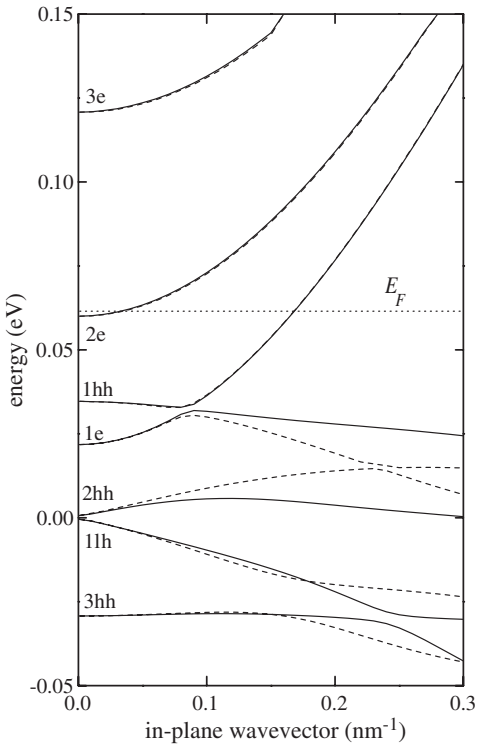

Figure 4. Subband dispersions as in figure 2 but with a bias of 0.25 V.

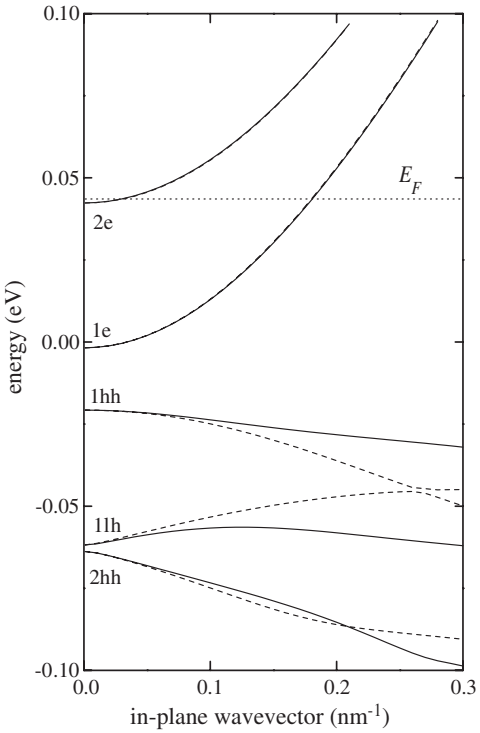

Figure 5. Subband dispersions as in figure 2 but with a bias of 0.4 V.

becomes larger than 0.3 V, all electron levels are above the hole levels, and the electron–hole system exhibits a typical normal semiconducting phase. This situation is shown in figure 5 for $V = 0.4$ V.

We notice that in figures 2, 4 and 5 in the energy region above the Fermi energy, the spin-splitting of each electron subband is negligibly small. On the other hand, below the Fermi energy the spin-splitting is significant, and the anticrossing behaviour is very complicated. Such a spin-splitting is caused by the spin–orbit interaction in asymmetrical quantum wells (Rashba effect). Due to the large spin-splitting of the hole-like levels, the different hole subbands approach each other and, hence, anticross at some non-zero in-plane wavevectors, as can be seen from figures 2, 4 and 5. Under a very high bias such as the cases in figures 4 and 5, the Fermi level is much higher than all hole-like states. In this situation there are no holes in the GaSb layer, and the calculated electron concentration is about 10^{12} cm^{-2}, which can be controlled by the applied bias voltages between the InAs/GaSb channel and GaSb contacts.

In summary, our theoretical calculation has reproduced the bias-induced semimetallic to hybridized-semiconducting phase transition and hybridized-semiconducting to normal-semiconducting phase transition which were observed experimentally [5]. The considered InAs/GaSb quantum wells are useful for the fabrication of mid-infrared lasers [12]. Such lasers have large optical matrix elements for the transitions between different electron-like and hole-like subbands because of considerable hybridization of the electron and hole states [12]. The external electric field can be used for tuning the emission frequency. The effects of phase transitions may critically influence the operation of such lasers. Notice also that we neglect

in our investigation the exchange interaction. Such interaction reduces the effect of Coulomb repulsion between electrons and between holes, because the exclusion principle tends to keep particles of parallel spin apart. The correction to the energy level positions is usually small in narrow-gap quantum wells made from InAs or InSb, but it becomes of the order of 10 meV in Si quantum wells [22]. However, even a correction of about 1 meV is of the order of the anticrossing gap energy in the hybridized-semiconducting phase and it can significantly influence the properties of the electron–hole system in the InAs/GaSb quantum well. This problem needs further investigation.

Acknowledgment

This work was financially supported by the Russian Foundation for Basic Research under grant No. 03-02-16788.

References

[1] Sai-Halasz G A, Esaki L and Harrison W A 1978 *Phys. Rev.* B **18** 2812
[2] Altarelli M 1983 *Phys. Rev.* B **28** 842
[3] Yang M J, Yang C H, Bennett B R and Shanabrook B V 1997 *Phys. Rev. Lett.* **78** 4613
[4] Lakrimi M, Khym S, Nicholas R J, Symons D M, Peeters F M, Mason N J and Walker P J 1997 *Phys. Rev. Lett.* **79** 3034
[5] Cooper L J, Patel N K, Drouot V, Linfield E H, Ritchie D A and Pepper M 1998 *Phys. Rev.* B **57** 11915
[6] Yang M J, Yang C H and Bennett B R 1999 *Phys. Rev.* B **60** R13958
[7] Marlow T P, Cooper L J, Arnone D D, Patel N K, Whittaker D M, Linfield E H, Ritchie D A and Pepper M 1999 *Phys. Rev. Lett.* **82** 2362
[8] Poulter A J L, Lakrimi M, Nicholas R J, Mason N J and Walker P J 1999 *Phys. Rev.* B **60** 1884
[9] Altarelli M, Maan J C, Chang L L and Esaki L 1987 *Phys. Rev.* B **35** 9867
[10] Naveh Y and Laikhtman B 1995 *Appl. Phys. Lett.* **66** 1980
[11] de-Leon S, Shvartsman L D and Laikhtman B 1999 *Phys. Rev.* B **60** 1861
[12] Halvorsen E, Galperin Y and Chao K A 2000 *Phys. Rev.* B **61** 16743
[13] Magri R, Wang L W, Zunger A, Vurgaftman I and Meyer J R 2000 *Phys. Rev.* B **61** 10235
[14] Zakharova A, Yen S T and Chao K A 2002 *Phys. Rev.* B **66** 85312
[15] Magri R and Zunger A 2002 *Phys. Rev.* B **65** 165302
[16] Zakharova A, Yen S T and Chao K A 2001 *Phys. Rev.* B **64** 235332
[17] Quinn J J and Quinn J J 1996 *Surf. Sci.* **361** 930
[18] Ko D Y K and Inkson J C 1988 *Phys. Rev.* B **38** 9945
[19] Burt M G 1992 *J. Phys.: Condens. Matter* **4** 6651
[20] Foreman B A 1997 *Phys. Rev.* B **56** R12748
[21] Zakharova A, Yen S T and Chao K A 2004 *Phys. Rev.* B **69** 115319
[22] Ando T, Fowler A and Stern F 1982 *Electronic Properties of Two-Dimensional Systems* (New York: American Physical Society)